Bollettino di Geofisica Teorica ed Applicata Vol. 53, n. 4, pp. 435-458; December 2012
DOI 10.4430/bgta0054

Early Pleistocene to late Holocene activity of the Magnola fault (Fucino fault system, central Italy)

P. Galli[1,2], P. Messina[2], B. Giaccio[2], E. Peronace[2], and B. Quadrio[2]

[1] *Dipartimento Protezione Civile Nazionale, Rome, Italy*
[2] *Ist. Geologia Ambientale e Geoingegneria, C. N. R., Montelibretti (Monterotondo), Italy*

(Received: July 4, 2011; accepted: December 16, 2011)

ABSTRACT. The Magnola Mounts (the Abruzzi, central Italy) are bound towards the Fucino Plain by a steep fault slope that is marked at its base by a continuous rock fault scarp (a "*nastro*", in Italian). In the Apennines, this particular feature is often interpreted *a priori* as evidence of Holocene tectonic activity, although sometimes climate-related exhumation processes or gravity-driven phenomena can generate such geomorphic markers. To unravel this possibility, we searched for field geological indications, and here report on our findings of both long-term and short-term evidence concerning the activity of the Quaternary Magnola fault. Paleoseismological analysis carried out across the talus resting against the rock fault plane revealed evidence of repeated surface rupture events from, and during, the Holocene, to historic times. Following a comparison of the ages of these events with those already known for the Fucino Basin faults, we argue that the Magnola fault acts as the north-western-most strand of the Fucino fault system, which is, in turn, the structure that was responsible for the devastating 1915, M_W 7, earthquake, as for other earthquakes in the past.

Key words. Active faults, paleoseismology, earthquakes, fault segmentation, fault interaction, central Italy.

1. introduction

After the 2009 L'Aquila earthquake [M_W 6.3, the Abruzzi, central Italy; Amato *et al.* (2011) and reference therein], what we definitely learned is that within the structural, lithological and climatic context of the central Apennines, the geological signature of seismogenic faults that are responsible for such, or larger, crustal events can be reasonably identified on the landscape surface. The morphological and/or tectonic indications can range from displaced Late Pleistocene deposits and forms, to rock-fault scarps carved into the substratum (known as "*nastri*" in the Italian literature), as with those that characterize the southwestern slopes of many mountain ranges in the Abruzzi (see Bosi, 1975). For instance, in the 2009 epicentral area, as well as faulted Pleistocene deposits and paleosurfaces, the evidence of recent fault activity can be seen in the presence of a discontinuous *nastro* that affects both the Mesozoic limestone and the Early Quaternary conglomerates [Paganica–San Demetrio fault system; PSDFS; see Fig. 1: Galli *et al.* (2010c, 2011)]. However, in this case, earthquake geologists have only collected these indications *ex post*, thus meaning that the seismic hazard related to the PSDFS has never been fully and correctly assessed.

On the other hand, if a fault is considered as active (e.g., Bartolini, 2010), in want of robust and integrated field geological constraints (stratigraphical, geomorphological, paleoseismological)

and analytical determinations (e.g., radiometric dating), there could be misleading implications in terms of regional seismic hazard assessment (e.g., Messina *et al.*, 2011a, 2011b). In this regard, where not supported by geological and analytical data, the presence of a fault *nastro* also cannot be considered as self-sustaining evidence of fault activity [see cases in Galadini (2006)], and *vice versa*. For instance, the active Mount Marzano fault system (southern Apennines; 1980, M_W 6.9 earthquake) has a discontinuous *nastro* that disappears along slopes that are covered by thick, secular beech forest. Here, this *nastro* is substituted by a compound scarp (*sensu* Slemmons, 1957) that is hidden and preserved below thick soils (Galli *et al.*, 2010a). The same ambiguity occurs along the neighboring Mount San Giacomo fault (Galli *et al.*, 2006), where the impressive *nastro* carved into the Mesozoic limestone disappears abruptly as the fault cuts through silicoclastic and /or dolomitic rock.

In the present study, we consider the WNW-ESE Magnola normal fault (hereafter MF). This has already been described in many studies, starting with Bosi (1975), who considered it reasonably active on the basis of its geomorphic imprint, i.e., the continuous fault *nastro* running along the base of the slope. According to Galadini and Galli (2000), the MF might be part of the Fucino fault system, which is the structure that was responsible for the strongest recorded earthquake in central Italy (1915, M_W 7). Thus, we believe that an understanding of Quaternary activity of the MF and its time/ space interactions with the other Fucino faults will represent a step forward in the characterization of the seismogenic behavior of this primary and very hazardous structure.

Through the integration of aerial photograph interpretations, field surveys, and geomorphological and paleoseismological analyses, we here cast light on this issue, and provide, for the first time, direct geological evidence for Pleistocene-Holocene activity of the MF.

2. Seismotectonic framework of the studied area

Since the Early Pleistocene, the Apennine fold-and-thrust belt of central Italy has been affected by NE-SW extensional processes [and/or gravitational collapse driven by uplift during crustal shortening: see Patacca *et al.* (2008)]. These processes are currently focused along the axis of the Apennine chain. Indeed, while the long-term geological signature of extension is revealed by the SW-dipping normal faults that bound the small-to-large intermontane basins (Galadini and Galli, 2000; Boncio *et al.*, 2004; Roberts and Michetti, 2004), its present rate is given by the calculated differential GPS velocities, which do not exceed 3 mm/yr in the area investigated (i.e., the Fucino region; D'Agostino *et al.*, 2011).

The active faults of the central Apennines have been systematically investigated through paleoseismological analyses over the past 25 years (Galli *et al.*, 2008; Fig. 1). These have been roughly grouped into two main systems: (i) the first runs along the chain axis (the Western fault system; i.e., Fig. 1, all of the faults except the Campo Imperatore fault system and the Mount Morrone fault system; CIFS and MMFS, respectively), to which the largest historical earthquakes have been associated and on which the present study is focused; and (ii) the second runs close to the eastern front of the chain (Eastern fault system; Fig. 1, CIFS, MMFS), which has been defined as historically silent (Galadini and Galli, 2000) as it has not generated known earthquakes in the past 1-2 ka, although it was active all through the Holocene.

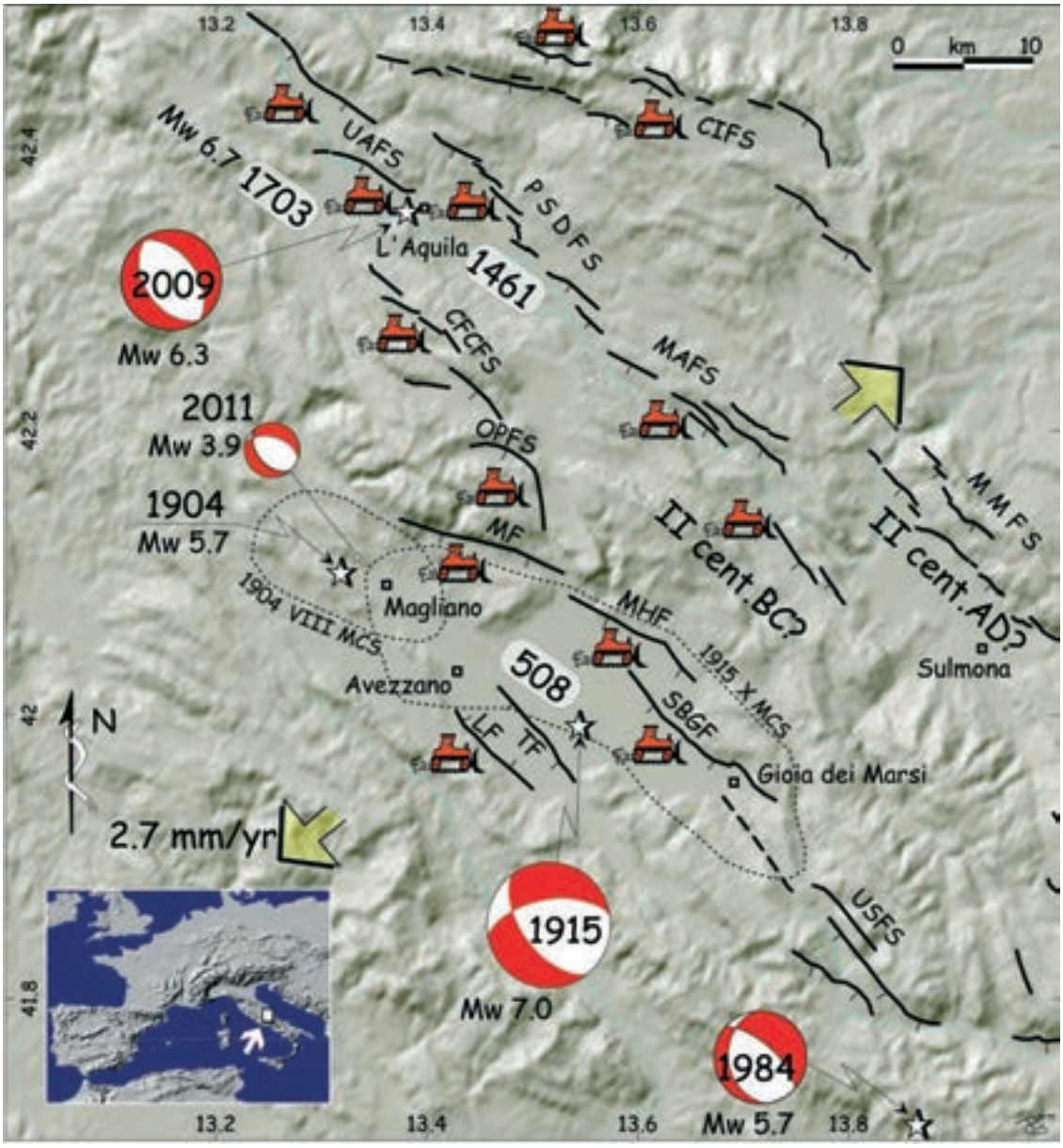

Fig. 1 - Digital terrain model showing the primary active faults of central Italy, and the main associated earthquakes [years in rounded rectangle; modified from Galli *et al*. (2010c)]. Arrows, extension from GPS velocity data (D'Agostino *et al.*, 2011). Bulldozer symbols, paleoseismological studies. The focal mechanisms are from Gasparini *et al.* (1985), SLU-EC (2011), Pondrelli *et al.* (2010). CFCFS, Campo Felice-Colle Cerasitto fault system; CIFS, Campo Imperatore fault system; LF, Luco dei Marsi fault; MAFS, Midde Aterno fault system; MF, Magnola fault; MHF, Marsicana highway fault; MMFS, Mount Morrone fault system; OPFS, Ovindoli Pezza fault system; PSDFS, Paganica-San Demetrio fault system; SBGF, San Benedetto dei Marsi-Gioia dei Marsi fault; TF, Trasacco fault; UAFS, Upper Aterno fault system; USFS, Upper Sangro fault system. Inset: Location of study area within Europe.

Primary normal faults are generally arranged into systems of 3-5 main *en-echelon* segments, each of which is 5 km to 20 km long (Bosi, 1975; Cello *et al.*, 1997; Galadini and Galli, 2000; Roberts and Michetti, 2004). With important exceptions, fault systems do not exceed 30 km in surficial length, and they are generally characterized by a 1-2 kyr recurrence time for M_W6.5 earthquakes (Galli *et al.*, 2008). Recently, this 'rule' has been challenged by the results of paleoseismological trenches that have been excavated in central-southern Italy. For instance, around L'Aquila (Fig. 1), the fault segmentation and fault linkage processes have fundamental roles in the seismogenic behavior of the primary structures (Galli *et al.*, 2010c, 2011). Here the PSDFS has been recognized as being responsible for both Mw ~6.3 (as the 2009 and 1461 earthquakes) and M_W 6.7 events. In this latter case, the PSDFS ruptured together with the adjacent Upper Aterno fault system (UAFS), as happened on February 2, 1703, and in other previous strong earthquakes. A similar seismogenic behavior can also be hypothesized for other normal fault systems of the Apennines, such as the aforementioned Mount Marzano fault system (Galli *et al.*, 2010a), and the Norcia fault system (Galli *et al.*, 2005). In contrast, shorter and/or more irregular recurrence times for M_W>6.5 earthquakes have been documented for the Aquae Iuliae fault (Molise, southern Italy; Galli and Naso, 2009), for the northern Matese fault system (Molise, southern Italy; Galli and Galadini, 2003), and again for the Mount Marzano fault system (Galli *et al.*, 2010b).

2.1 The Fucino seismogenic structures

The MF falls within the epicentral area of the strongest earthquake in central Italy [January 13, 1915; M_S 7.0; I_0 XI MCS; more than 30,000 fatalities: Margottini and Screpanti (1999) and Molin *et al.* (1999)]. This event was generated by the Fucino fault system (Galadini and Galli, 1999), which is an array of NW-SE normal faults that dip mainly SW. According to eyewitnesses (Serva *et al.*, 1988; Galadini *et al.*, 1995, 1997, 1999), surface faulting occurred all along the faults surrounding and/or inside the Fucino plain (i.e., San Benedetto dei Marsi-Gioia dei Marsi and Marsicana Highway master faults, synthetic and antithetic splays of Trasacco fault and Luco fault; Figs. 1 and 2, respectively, SBGF, MHF, TF and LF). Oddone (1915) followed the fault (Fig. 3) from beyond Gioia dei Marsi (to the extreme SE) to Magliano dei Marsi (to the NW), for a total length of *ca.* 33 km along a NW-SE direction (Fig. 1). Other clues from newspapers (Corriere d'Italia, 1915; Corriere di Napoli, 1915; Gazzetta del Popolo, 1915; Il Mattino, 1915; Osservatore Romano, 1915) reported on the opening of a large "*crepaccio*" (vent) on the Mount Velino slopes, which would tentatively indicate surface faulting along the Magnola rock-fault scarp. On the basis of these reports, and of the "highest intensity datapoint distribution" (Fig. 1), Galadini *et al.* (1998) hypothesized that the 1915 earthquake was generated by the contemporary slip of the MF-MHF-SBGF (all together giving a *ca*. 37-km-long structure), with rupture directivity from the SE towards the NW (Berardi *et al.*, 1999; Galli *et al.*, 2002). The 1915 surface rupture was also recognized inside 15 paleoseismic trenches in the plain (Michetti *et al.*, 1996; Galadini *et al.*, 1997; Galadini and Galli, 1999), which revealed many other previous surface rupture events with offsets comparable to the 1915 one. In particular, Galadini and Galli (1999) identified a penultimate event in a time span between 426 AD and 782 AD (see details in Galli *et al.*, 2008), which was referred to an earthquake that hit Rome in 508 AD. Prior to this, there was another between 3500 BP and 3300 BP (1450 BC in Galli *et al.*, 2008), another previously

Fig. 2 - Expanded digital terrain model from Fig. 1 of the Fucino fault system, which was the structure responsible for the M_w ~7 earthquakes of 1915, 508 AD, and many previous paleoseismic events. The main faults bounding at the NE of the Fucino basin are in bold blue (the Magnola, Marsican Highway, and Gioia dei Marsi-San Benedetto dei Marsi faults). The main synthetic (Trasacco), antithetic (Luco dei Marsi) and transversal (Tre Monti) faults are in blue. Note at the NW tip of the Magnola fault the epicentres of the M_w 5.7, 1904 and the M_w 3.9, 2011 earthquakes. The darker area fits the rough surface projection of the in-depth seismogenetic structure. Bulldozers are paleoseismological sites where paleoearthquakes have been identified [see text and Galli *et al.* (2008)]. Focal mechanisms are from Gasparini *et al.* (1985) and SLU-EC (2011). Dashed rectangle shows area of Fig. 5.

between 5944 BP and 5618 BP (3831 BC in Galli *et al.*, 2008), and previous occurred between 12729 BP and 7576 BP, between 12729 BP and 12053 BP, between 17666 BP and 16397, and between 19750 BP and 18450 BP. Obviously, due to possible stratigraphical hiatus, not all of the reported events were necessarily strictly consecutive, especially the older ones.

It is worth noting that the only other important historical earthquake in the hangingwall of the Fucino fault system [see Table 1 in Molin *et al.* (1999)] occurred in 1904, which caused the destruction of Magliano dei Marsi and other neighboring villages (M_S 5.5; I_0 8.5 MCS; Spadea *et al.*, 1985; Margottini *et al.*, 1993. M_W 5.7 in the current Italian catalogues). A long chasm with an associated light offset was also observed in the foothill of Velino-Magnola Mounts (Il Giornale d'Italia, 1904), even if the conciseness of the account does not allow it to be related to surface faulting phenomena. However, considering that the mesoseismic area (I_S >7.5 MCS) is elongated along the NW-SE within the hangingwall of the MF (Fig. 1), Galadini *et al.* (1997) hypothesized

Fig. 3 - Original photograph of Oddone (1915) of the surface faulting effects near San Benedetto dei Marsi from the 1915 Fucino earthquake.

that in 1904 a portion of the MF slipped, priming the entire rupture of the Fucino fault system in 1915. Even if we ignore the 1904 focal mechanism, we could hypothesize that it was similar to the one calculated for an event that occurred in 2001 very close to its epicenter (M_W 3.9; Figs. 1, 2), which shows a NW-SE extensional mechanism.

Finally, Bagh *et al.* (2007) identified a small sequence (in the period of 2003-2004) in the hangingwall of the MF with SW-down-dip fault kinematics, which was nucleated from 10 km to 15 km in depth; they associated this to the deepest portion of the MF [see Bagh *et al.* (2007) and, Fig. 4e].

Table 1 - Radiocarbon dates of organic sediment samples collected in the trench dug across the Magnola Fault, as defined by accelerator mass spectrometry (C.I.R.C.E. laboratory, Caserta). The 2σ calibration were carried out using the Calib 6.0.1 program (Stuiver *et al.*, 2010).

Trench	Sample	Analysis	Dated material	Measured Radiocarbon Age (BP)	2σCalibration	Fault	Referencs
1	MAGN01	AMS	Organic sediment	8611 ± 48	9695-9501 BP	MF	this paper
1	MAGN02	AMS	Organic sediment	5790 ± 80	6408-6752 BP	MF	this paper
1	MAGN03	AMS	Organic sediment	1710 ± 26	255-401 AD	MF	this paper

Fig. 4 - View looking west of the Early Pleistocene breccias ("Bisegna" or "mortadella" breccias) in the footwall of the Magnola fault (photograph by PG).

3. Geological hints for Pleistocene activity of the Magnola fault

3.1 Previous studies

Piccardi *et al.* (1999) carried out structural and geomorphic analyses along the fault that they assumed to be active and 15 km long. Making the crude assumption that the glacial smoothing of the mountain slope ceased at 14 ±4 ky BP, Piccardi *et al.* (1999) concluded that the vertical throw that they measured across the fault *nastro* yields an average postglacial slip-rate of 0.7 ±0.3 mm/yr. On the other hand, Gori *et al.* (2007) hypothesized that the layered breccias at *ca*. 1900 m a.s.l. in the footwall of the MF (Fig. 4) might be the remains of an Early Pleistocene alluvial fan that lies over an old pediment, and that both were lowered by the fault in the hangingwall at 1,200 m a.s.l., where similar breccias outcrop. Assuming an age of 1.0 ±0.2 Ma for the breccias, these provide a long-term slip-rate of 0.54 to 0.81 mm/yr (*n.b.*, this value does not take into account the primary down-slope dip of the breccias).

Palumbo *et al.* (2004), Schlagenhauf (2009) and Schlagenhauf *et al.* (2010, 2011) carried out cosmogenic ^{36}Cl dating on carbonate samples along the exhumed fault plane. According to Palumbo *et al.* (2004), the distribution of the *in-situ* ^{36}Cl concentrations was best explained by five successive earthquake surface ruptures that occurred 12 ky, 10.5 ky, 7.4 ky, 6.7 ky, and 4.85 ky BP (these dates would imply a vertical slip rate of 0.58 mm/yr). However, Schlagenhauf (2009) refined the modeling of the content of *in-situ* ^{36}Cl cosmonuclide on the same samples as Palumbo *et al.* (2004), and added many others that came from the buried portion of the same

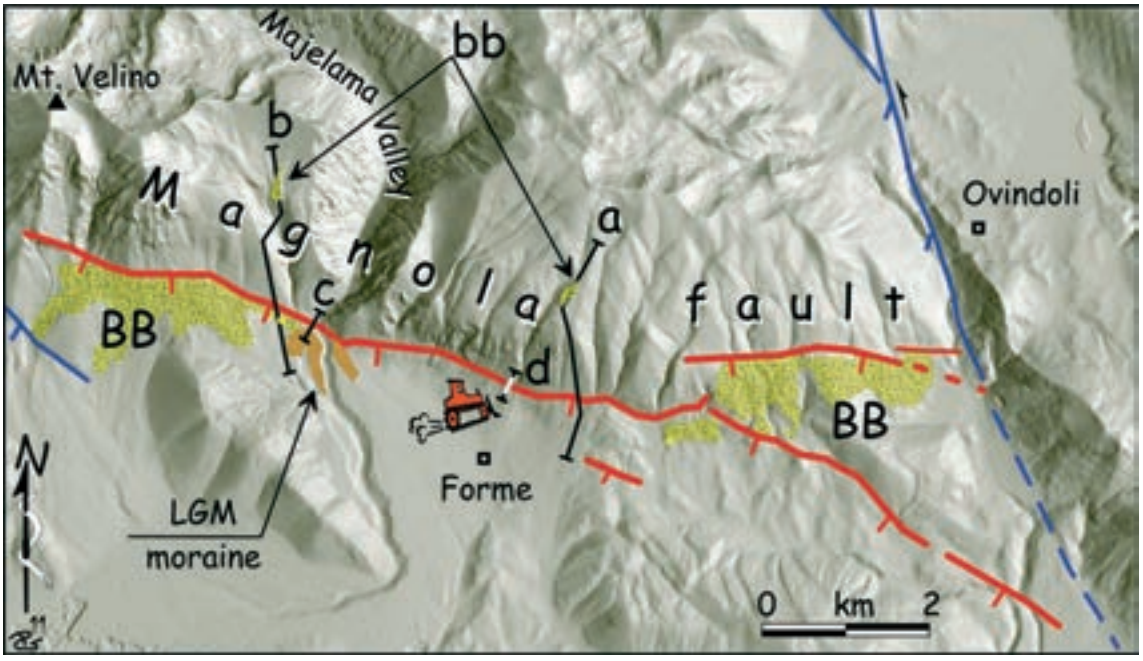

Fig. 5 - High-resolution digital terrain model of the area indicated in Fig. 2. BB and bb, "Bisegna" breccias (footwall and hangingwall, respectively). a-d, geological sections in Figs. 6, 8A, and 10. Bulldozer symbol, the paleoseismological site. Note the flat, top-surface shape of the vast LGM fluvioglacial fan exiting the Majelama Valley, southward.

plain, and from four other sites. These nine paleo events occurred at *ca*. 13.7 ky, 10.7 ky, 9.2 ky, 8.5 ky, 7.4 ±1.8 ky, 4.8 ±0.8 ky, 3.8 ±0.9 ky, 3.3 ±0.7 ky and 1.1 ±0.6 ky BP. Schlagenhauf *et al.* (2010) then recalculated the ages of the last five events at 7.2 ±0.5 ky, 4.9 (+0.7/–0.9) ky, 4.0 (+0.8/–1.1) ky, 3.4 (+0.5/–0.9) ky and 1.5 (+0.5/–0.9) ky BP, each one with an offset between 1.6 m and 3.6 m, and with a consequent vertical slip rate in the past 7 ky of 1.2 mm/yr. Finally, in considering also the data gathered on the Velino fault, Schlagenhauf *et al.* (2011) proposed again the occurrence of the following nine events: 14.7 ±1.0 ky, 11.0 ±0.5 ky, 10.1 (+0.4/–0.5) ky, 9.7 (±0.5/–0.3) ky, 7.8 (±0.7/–0.8) ky, 4.8 (±0.3/ ±0.4) ky, 4.4 (±0.3/ ±0.4) ky, 4.0 (+0.4/±0.5) ky, 1.3 ±0.4 ky BP.

It is worth noting here that the basal Mount Velino structure represents a didactic example of fault-inversion of a Messinian thrust ramp. Today, its main morphological character is a flat hillslope that is carved into the low-angle fault plain that, in turn, was reactivated in extension during the Early Pleistocene (Nijman, 1971; Bosi *et al.*, 1994). Anyway, according to Chiarini *et al.* (1997), the normal fault was sealed by Middle Pleistocene paleosurface, and thus contrary to what was claimed by Schlagenhauf *et al.* (2011), it should be considered no longer active.

3.2 New field data

To provide field geological evidence of recent surface faulting, if any, and to eventually quantify the Pleistocene MF activity, we carried out a geological and geomorphological survey all along the southern slopes of the Magnola Mounts. On a digital terrain model of the area with

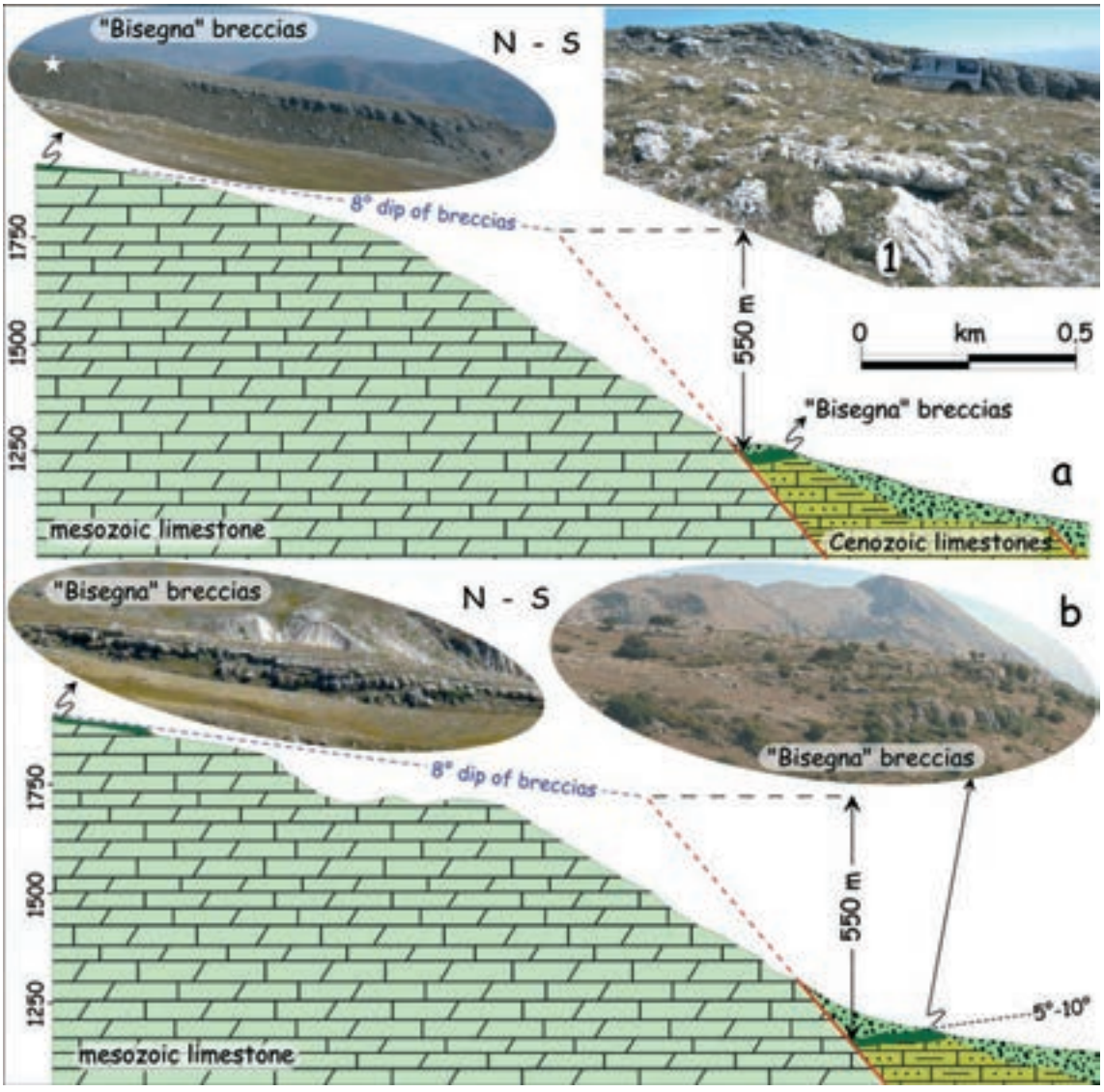

Fig. 6 - Geological sections (a-b in Fig. 5) showing the total offset of the "Bisegna" breccias along the SW Magnola Mounts slope. Note in the upper right the carbonate substratum (1) below the breccias in the Magnola fault footwall (white star in the upper left picture, site of Fig. 4. Photographs by PG).

a 5-m-spaced grid (from 1:5,000 data of Regione Abruzzo, 2010), and through interpretation of aerial photographs and GPS-based field surveys, we first traced the different segments and splays of the MF (Fig. 5). The 8.5-km-long, western segment outcrops continuously, with an average N107° strike; this then splits into two strands, one 5-km-long and with a N117° strike, and the other 3-km-long with a 90° strike in the footwall. Although the fault *nastro* disappears as it goes SE, it points directly towards the NW tip of the MHF, and thus joins the eastern primary Fucino structure. In turn, in the NW, it ends abruptly against the above-mentioned Mount Velino N130° basal fault (Fig. 2) that appears to act as a barrier that has inhibited the growth of the MF

Fig. 7 - Photograph of view looking north of the fault scarp carved into the LGM moraine at the mouth of Majelama Valley. Arrows, top of the moraine crest, displaced at least 7 m by the fault (photograph by PG).

westwards.

Then we surveyed and mapped the sparse "*Bisegna*" breccias outcrops (*sensu* Bosi and Messina, 1991; "*brecce mortadella*" *sensu* Demangeot, 1965; "*brecce di Fonte Vedice*", *sensu* Bertini and Bosi, 1993; see also Bosi *et al.*, 2003, and references therein). Indeed, as this is the only correlative Quaternary unit that outcrops across the fault, in agreement with Gori *et al.* (2007), we decided to use it as a long-term indicator for the MF slip rate. In the footwall, there were only two relics of the original clastic succession (Fig. 5, bb) which lie over a gently dipping paleosurface that is still visible between 1850 m and 2000 m a.s.l.. The easternmost of these is made up of a 10-15-m-thick, and less than 350-m-long and 100-m-wide isolated slab of well stratified breccias, which outcrop between 1920 m and 1875 m a.s.l. (Figs. 4 and 6); the westernmost, and smaller, of these outcrops is within the same elevation range (Figs. 5 and 6), and both of them lie unconformably over the marine Mesozoic limestone (Fig. 6, upper-right panel). The top surface of these slabs dips downhill by 8° to 9°, which matches with the average dip of the breccias strata (Figs. 4 and 6); i.e., with the primary depositional dip of the gravel. In turn, the strata measured in the widespread outcrops of the hangingwall (Fig. 5, BB) dip northwards by 5° to 10° as they approach the fault (i.e., they are tilted counter to the hill by 15°-20°), whereas they crop out sub-horizontally going southwards. In the hangingwall, their thickness is 3-4 times that measured in the footwall, and so we believe that the fault onset is coeval to the clastic deposition, even if we cannot exclude that a higher rate of erosion in the footwall has strongly reduced their original thickness. However, in this case, we would assume that erosion - by chance - has proceeded parallel to the primary stratification.

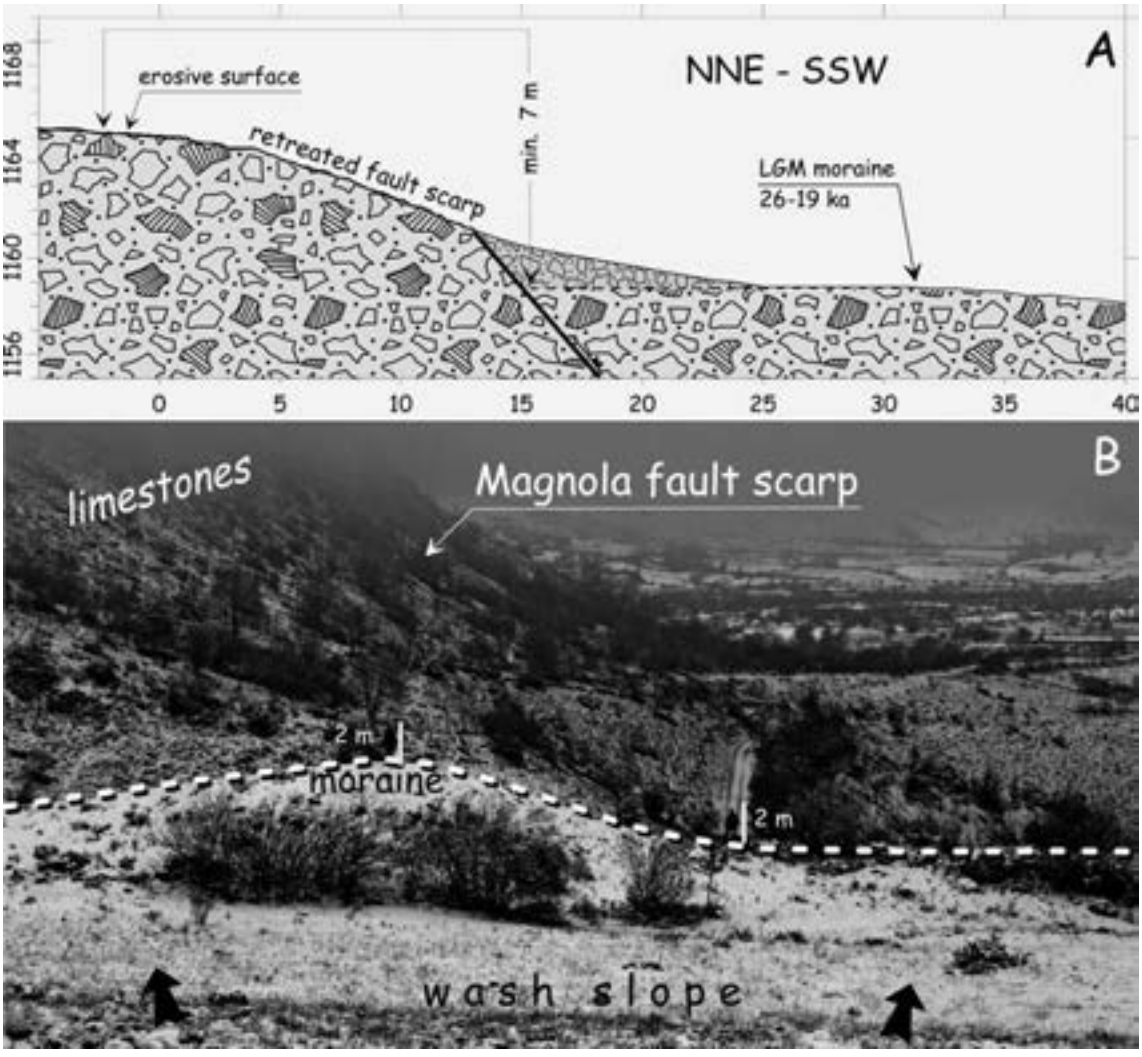

Fig. 8 - LGM moraine at the mouth of the Majelama Valley. A. geological section of the faulted crest of the moraine from Fig. 5c. Note that the top surface in the footwall has been eroded, and thus the measured offset is at a minimum. B. Photograph of downhill view looking SE of the faulted moraine (two people included for scale; photograph by PG).

On this background, and considering the reciprocal dip of fault and deposits, the net offset of the breccias bottom that we evaluated along two geological profiles across the fault is 550 m (Fig. 5, traces a and b, and Fig. 6).

We also mapped the last glacial maximum (LGM) moraine deposits that are affected by the MF at the mouth of the deeply entrenched Majelama Valley (1200-1100 m a.s.l.; Frezzotti and Giraudi, 1992; Fig. 5). The moraine is made up of massive and etherometric gravel in a coarse sandy matrix, and it shows a prominent fault scarp carved into the relic of the original periglacial forms (Figs. 7 and 8B). Although the footwall portion has been strongly reshaped by erosional processes that have resulted in the truncation of the moraine top surface, we estimate a minimum post-LGM offset of 7 m along a high-resolution topographic profile (Fig. 5c) carried out across

Fig. 9 - Photograph of view looking W of the Late Pleistocene faulted conglomerates (dashed line, one of the splays) at the apex of a fan crossing the Magnola fault. Note on the right the main fault plane exhumed by the deep, recent gully erosion (area of Forme village; PM piggyback of Donkey included for scale; photograph by PG).

the fault scarp (Fig. 8A).

The Late Pleistocene activity of the MF is also confirmed by the faulting of the uppermost layers of the fan/ talus deposits resting against the rock fault plane. This can be seen within the entrenched apex of the post-LGM alluvial fans (Frezzotti and Giraudi, 1992), which open out at the mouth of some streams that dissect the carbonate slope, as for the one north of Forme village, where some synthetic splays outcrop a few meters from the *nastro* (Fig. 9). West of this fan, we carried out three high-resolution topographic profiles (Fig. 5, site d), along the slope and across the fault *nastro* (Fig. 10). By intersecting the projection of the slope profile measured in the footwall (i.e., uphill of the retreated scarp) with the fault plane projection, we extrapolated the slope profile that might have existed during the strong LGM rhexistasy phases (Fig. 10, dashed lines). This, we assume, was when the slopes and the fault scarps were smoothed and rectified (Dramis, 1983; Roberts and Michetti, 2004). We noted that the height of the scarp (the *nastro* plus the retreated fault scarp) along this portion of the fault is relatively constant in all of the profiles, with a vertical offset cumulated by the fault of *ca*. 16 m. Indeed, as discussed below, this is an overall value that should have an unquantifiable amount deducted, due to the erosive processes that occurred during the Holocene (i.e., the exhumation processes of the *nastro*).

4. Paleoseimological analysis

To ascertain, and possibly constrain, the Holocene fault activity, we carried out paleoseismological analyses by exploiting the trench opened by Schlagenhauf (2009) for cosmogenic ^{36}Cl dating on the buried portion of the carbonate fault plane (Fig. 5, site d). Indeed,

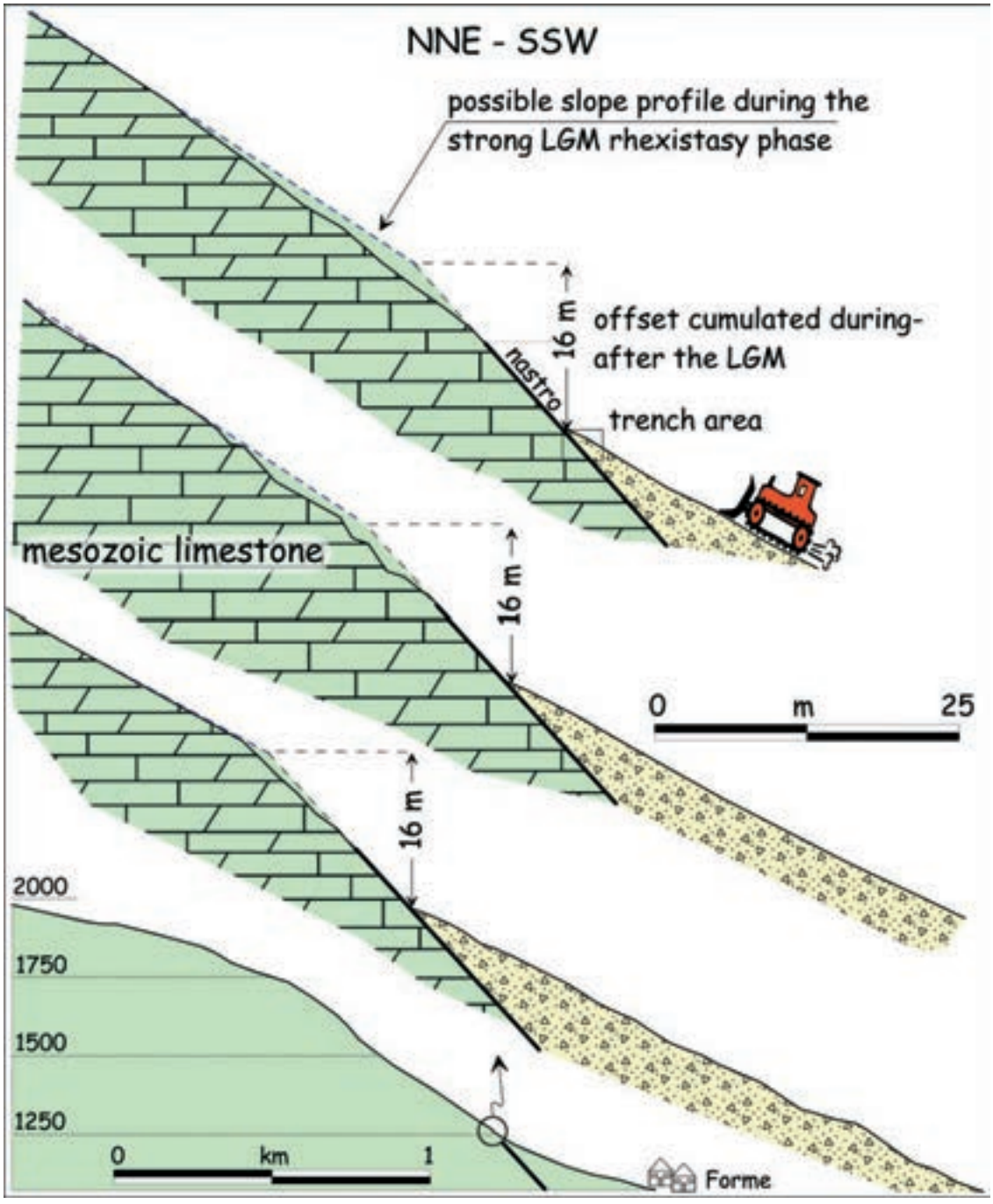

Fig. 10 - Geological sections from Fig. 5d, showing the offset of the slope profile across the Magnola fault nastro. Note that the height of the nastro is roughly half of the total offset, and that part of the offset might be due to talus erosive processes at the bottom of the nastro. Lower panel, the profile positions along the whole Magnola Mounts slope from Fig. 6a.

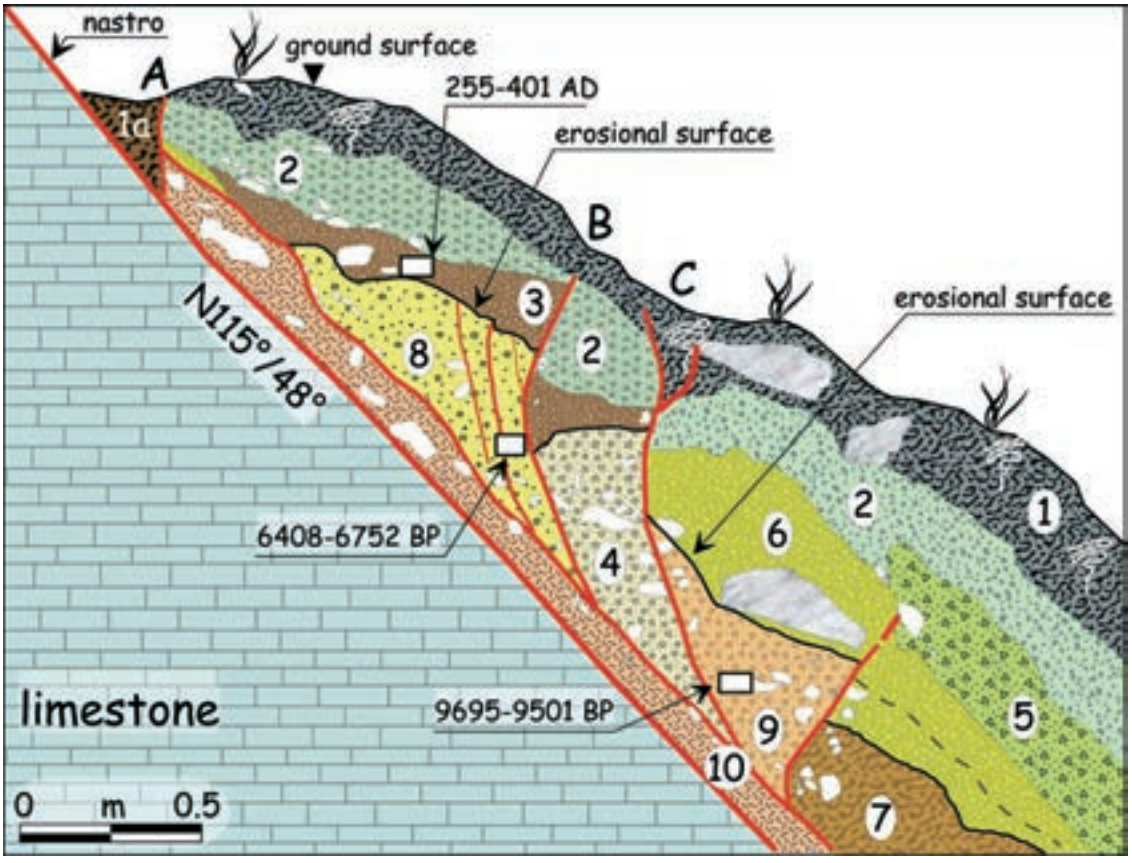

Fig. 11 - Log of the paleoseismological trench analysed, as for Fig. 5d and Fig. 10, upper panel. All the deposits are displaced and dragged along the fault nastro, indicating the occurrence of repeated surface faulting events up to historic times (e.g., 508 AD, 1915 earthquakes). 1, brownish sand and silt with carbonate clasts (presently forming soil; 1a, wedge of brownish sand and silt); 2, fine angular gravel, in orange sandy matrix; 3, brownish sand and silt with carbonate clasts (à borted' paleosol); 4, massive badly sorted gravel in abundant reddish silty matrix; 5, massive badly sorted angular carbonate gravel; 6, faintly stratified, angular classed gravel; 7, massive badly sorted gravel in abundant reddish silty matrix; 8, wedge of massive badly sorted angular carbonate gravel in brownish sandy matrix; 9, wedge of massive badly sorted angular carbonate gravel in reddish-brownish sandy matrix; 10, chaothic silty deposit, packed and dragged along the fault. See text for further details.

after re-digging and enlarging the E wall of the trench, we built up a 0.5 net and logged at 1:20 scale the exposed slope-derived succession, which is entirely faulted against the carbonate *nastro* (here striking N115°, with a dip of 48°; Figs. 11 and, 12). All of the depositional units that we recognized are affected by secondary splays that branch from the main plane, i.e., from an *ca*. 10-cm-thick chaotic silty material (shear zone) that is packed and dragged between the flat carbonate fault plane and the wedge of clastic deposits (Fig. 11, unit 10). The splays cut the whole slope-succession, as they are partly sealed by the present humic horizon (Fig. 11, unit 1). Apart from this latter unit, and unit 3, which is a thin, scarcely developed paleosol (Fig. 11), all of the others units (units 4-9) are massive or faintly stratified (unit 6) angular, badly sorted gravels, in reddish silty matrix (very abundant in units 4 and 7; Fig 11). The complex primary relationships among

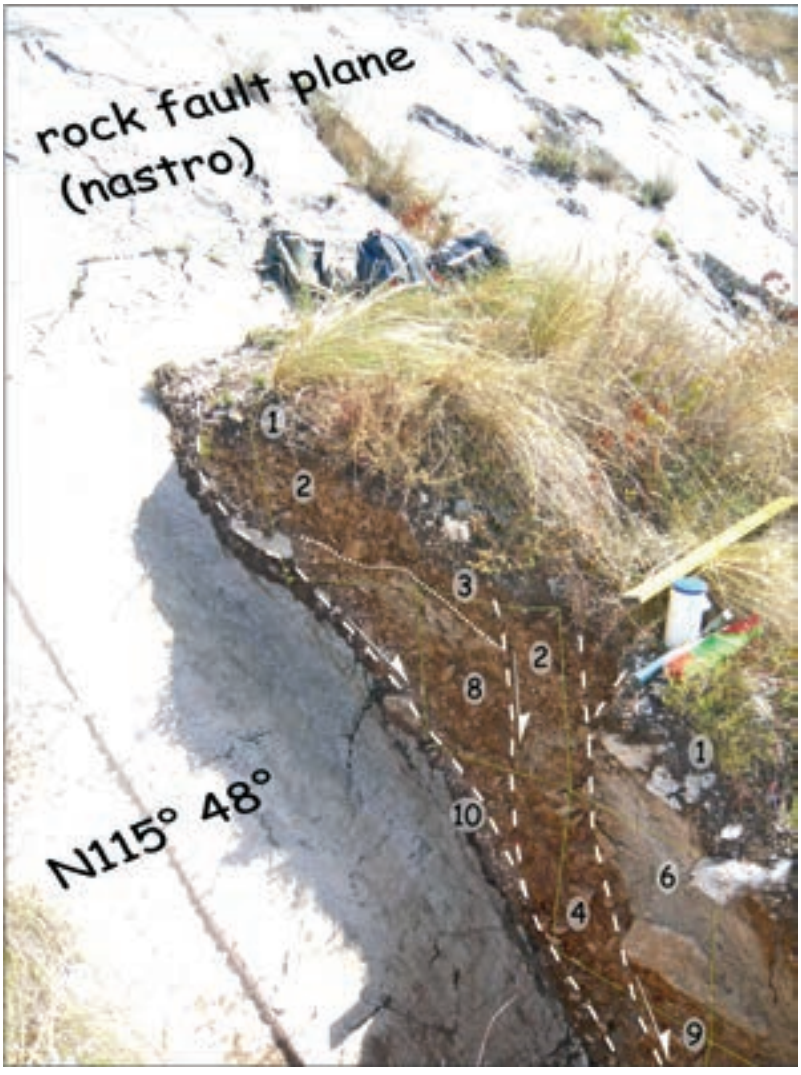

Fig. 12 - Photograph of oblique view looking NE of the eastern wall of the paleoseismological trench of Fig. 11. Labels as in Fig. 11. Dashed lines indicate some of the visible fault splays. The net is 0.5 m (photograph by PG).

these different units have been deeply skewed by the tectonic/ gravity-driven deformation that has affected the talus, which makes it difficult to reconstruct the original stratigraphic framework. However, as the entire succession has been faulted repeatedly in recent times, to constrain the age of these events, we sampled and dated the organic matrix of some of the units.

Samples MAGN01 and MAGN02 (Table 1) are from units 9 and 8, respectively (i.e., gravelly colluvia in reddish-brown sandy matrix), and these provide the age of their parent material (i.e., before it was colluviated downwards on the slope). They thus roughly indicate the "*terminus post quem*" for their deposition, which is the Late Holocene. We can argue that this happened after the phase of slope stability and pedogenesis recorded in the central Apennines up to *ca*. 4.5 ka; i.e. during the Neoglacial period (Giraudi *et al.*, 2011). However, what is more striking is the age of unit 3 (sample MAGN03), which falls fully into the Roman Imperial period. Unit 3 is a thin,

immature paleosol laying on an erosional surface that, in turn, truncates the different units below (e.g., units 4 and 8). Unit 3 is buried by fine angular gravels (unit 2), and both are faulted once (Fig. 11, fault splay B). The age of unit 3 is consistent with the 'short' humid sub-phase of soil-stability that was recorded during the Late Roman age [150-350 AD; e.g., in Martin-Puertas *et al.* (2009)], before the cold and arid successive period that probably 'aborted' the soil. Units 2 and 3 have been successively buried/ pedogenized by unit 1, which looks, however, to have been involved in successive deformational events that have led to the opening and filling of a wedge (Fig. 11, 1a) that rests between the slope-succession (Fig. 11, splay A) and the *nastro*. This further event is also confirmed by the offset of unit 1 on the splay C, and by its faint thickening in the hangingwall.

Therefore, we can hypothesize that a penultimate faulting event occurred not much after 255-401 AD (i.e., after the burying of paleosol 3), and a final faulting event that involved the presently forming humic horizon (unit 1).

Finally, a further previous event that affected the Neoglacial colluvia is also visible, and this is sealed by the above-mentioned erosional surface that lies below the Roman level (i.e., unit 3).

5. Discussion

On the basis of the ages of the Quaternary deposits that have been affected by the MF, and of the different offsets calculated for each of these, it is now possible to obtain: 1) the fault slip-rate, both over the long-term and the short-term; 2) the extension rate across this sector of the Apennines; and 3) the ages of some of the paleoearthquakes observed in the trench. Finally, we can provide a hypothesis concerning the seismogenetic behavior of the Fucino structure.

5.1. Long-term slip rates

The geological sections traced across the SW slope of the Magnola Mounts (i.e., the long-term expression of the cumulated fault scarp; Figs. 5, 6, a, b) show that the continental breccias are offset by 550 m, for both the western and central parts of the fault (no breccias in the footwall of the easternmost tip). According to Bosi *et al.* (2003), these breccias are datable to around 1.0 ±0.2 Ma, as they would represent a ubiquitous deposit of the central Apennines that probably formed during one climatogenic event (see also D'Agostino *et al.*, 1997). Recently, we surveyed similar *facies*-equivalent rudites around L'Aquila, where they also interdigitate with whitish lacustrine silts that are characterized by reversed paleomagnetic polarity (Matuyama epoch, 0.78-1.77 Ma; Giaccio *et al.*, 2011). As these silts contain a cluster of tephra layers that are petrologically attributable to the calc-alkaline Tuscany Province (i.e., they lack K-felspars and/or leucite crystals), and considering that the explosive activity of the Cimini Volcano was the only one that was potentially capable of generating widespread tephra clouds, we tentatively suggest an age around, or slightly subsequent to, 1.35 Ma to 0.90 Ma (Peccerillo, 2005) for the breccias deposition, which confirms the hypothesis of Bosi *et al.* (2003). Therefore, assuming this age of 1.0 ±0.2 Ma, we calculated a vertical slip-rate of 0.6 ±0.1 mm/yr. Indeed, this rate should be considered as a minimum, as we do not know when the fault started its activity. However, as the breccias are always much thicker in the hangingwall than in the footwall (i.e., across the fault), it is reasonable to hypothesize that the fault was already active during the breccias deposition.

Therefore, although it might have varied in time, we would say that this slip-rate is a reliable average value for the past ~1 Ma.

5.2 Short-term slip rates

Unfortunately, the absence (i.e., the erosion) of other younger deposits hampers further evaluation concerning the fault activity during the Middle and Upper Pleistocene, whereas we have data for the end of the Late Pleistocene–Holocene, up to historic time. For instance, as far as the LGM faulted moraine at the mouth of the Majelama Valley is concerned, we have inferred a 0.3 mm/yr slip rate after the presumed end of the glacial shaping (Figs. 6, 8 profiles). For this, we need to bear in mind that in the highest mountains of central Italy the maximum extent of the glaciers was already reached before *ca*. 23 ka, whereas the glacial retreat began *ca*. 22 ka, when thick outwash sands and gravels deposited (Giraudi, 2004). We consider this slip rate as a minimum, as the thin crest of the moraine in the footwall has been eroded by an amount that cannot be quantified, which thus hampers the evaluation of the whole offset.

A less robust indication for the quantification of the activity rate of the fault in recent times can be derived from geomorphological considerations. The geological sections made on the high-resolution topographical profiles across the fault *nastro* (the central portion of the MF; Fig. 10) showed that the vertical offset of the original slope surface that possibly formed during the strong LGM rhexistasy phase is 16 m. In reality, this offset should be added to by the thickness of the post-LGM colluvia that was deposited in the hangingwall (Fig. 11, *ca*. 2 m). Half of this offset is roughly accounted for by the vertical height of the *nastro* itself, whereas the other half is accounted for by the rocky retreated scarp uphill. If the ages provided by Schlagenhauf *et al.* (2011) at the top of the *nastro* in this area are reliable (*ca*. 8 kyr), regardless of the number and dating of their proposed faulting events, this would suggest that half of the post-LGM offset has cumulated in the past 8 ka, whereas the other half has cumulated during the preceding period. All of these considerations yield a Holocene vertical slip rate of 0.9 ±0.1 mm/yr, which would be the highest rate in central Italy (e.g., in Galadini and Galli, 2000).

However, as mentioned above, we are relatively skeptical when we consider that the whole measured vertical offset across the *nastro* is due to only post-LGM coseismic surficial slip. Although the above-mentioned assumption made by Dramis (1983) concerning the regularization of the areal slopes during the LGM in central Italy has been indirectly strengthened through physical models that simulate the effects of the periglacial erosion processes on the degradation of slopes and scarps (Font *et al.*, 2006; see also Murton *et al.*, 2006, for physical modeling of limestone fractures by gelifraction in seasonal frost), we must bear in mind two different factors that make things more complicated, as follows.

First of all, we have to consider that part of the presently measured offset cumulated not only after, but also during the local LGM rhexistasy phase (*sensu* Erhart, 1951; Castiglioni, 1979), which is a time span that partly exceeds the LGM bounds derived simply from the relative sea levels (i.e., 26.5-19.0 ka; Clark *et al.*, 2009). Indeed, south of the mouth of Majelama Valley, the vast fluvioglacial alluvial fan that characterized this cold and partly arid rhexistasy phase took place after 30 ka, and before 19415 BP to 15442 BP (2σ cal. age, recalibrated from Frezzotti and Giraudi, 1992), a time span during which the glacial tongue reached a length of 6 km here. In this period, seasonal gelifraction processes and areal debris flow will have smoothed the slopes of the

Magnola Mounts, although this will have happened in competition with the growing basal fault scarp. Therefore, we cannot quantify how much of the vertical offset across the retreated fault scarp (let us say, at least the 8 m measured above the *nastro*) formed after or during the LGM. Conservatively, we can conclude that the 16-m-offset (plus *ca*. 2 m of colluvia piled on in the hangingwall) has cumulated in the past 30 ka, which implies an overall vertical slip-rate of 0.6 mm/yr.

Nevertheless, the second factor that we must take into account is the exhumation of the fault *nastro* due to differential erosive processes at the limestone-debris interface (e.g., Bartolini, 2010), as seen by those inside the several gullies, where the rock fault plane outcrops for a dozen meters (Fig. 9). Indeed, during the cold and arid climate phases of the Holocene, the lack of stable soil, the cryoturbation phenomena, and the strong, episodic rainfall (with heavy water-flow on the *nastro*) eroded the loose debris that rested at the foot of the rock fault scarp. This probably happened mainly during the stadial phases [e.g., Younger Dryas, or Mount Aquila stadial in the central Apennines; 10-11 ky BP; Giraudi (2004)], and/or during the so-called Neoglacial phase, which began roughly after 4.5 ky BP (Giraudi *et al.*, 2011). This is also supported by the dating and the nature of the deposits in the paleoseismological trench (Fig. 11), where the age of the parent material of the colluvia predates the Neoglacial. These deposits are then truncated upwards by erosional surfaces, which will have removed the younger deposits. An immature soil only developed during part of the Late Roman period (Fig. 11, unit 3), which prevented further erosion of the *nastro*.

Therefore, the vertical offset measured across the *nastro* that we previously tentatively referred to the past 8 ka also contains an amount due to erosion, and thus the previously mentioned slip-rate of 0.9 mm/yr must be considered an extreme boundary. Analogously, we believe that the age of some of the slip-events that Schlagenhauf *et al.* (2011) hypothesized through their cosmogenic ^{36}Cl dating of the *nastro*, together with their relatively large offsets, are not co-seismic *tout court.* For instance, the cluster that Schlagenhauf *et al.* (2011) put just between 5-4 ky BP fits with the beginning of the Neoglacial period, when strong erosion related to the cold climate probably contributed to the *nastro* exhumation.

5.3. Extension rate

From all of the above, it appears that the MF has been active at least since the end of the Early Pleistocene, with an average vertical slip rate of 0.6 ±0.1 mm/yr. This value fits in with that evaluated across the MHF, where Galadini and Galli (2000) calculated a minimum slip-rate of 0.4 mm/yr for the past 0.4 Ma. During the end of the Late Pleistocene and in the Holocene, the MF rate will have been higher than 0.3 mm/yr, and lower than 0.9 mm/yr, which can be assumed as 0.6 mm/yr. In terms of the pure NE-SW extension, this provides a value that ranges between 0.4 mm/yr and 0.5 mm/yr, depending on the fault dip at depth (60°-50°, respectively), which is *ca*. 15% of that which D'Agostino *et al.* (2011) measured through geodesy across the whole Western fault system and Eastern fault system (2.7 mm/yr; Fig. 1, yellow arrows). If we assume tentatively a similar extension rate also across the silent Eastern fault system, and eventually also across the intermediate Middle Aterno fault system (Fig. 1, MAFS), the GPS velocities are anyway twice those related to the faults. This might simply mean that *ca*. half of the currently ongoing extension in the upper crust of central Italy can be accounted for by fragile tectonics (mostly during M_w >6.3 earthquakes on the

primary faults), while the other half can be accounted for by diffuse ductile or semi-fragile deformation, which is not resolved by surface geology (see discussion in D'Agostino *et al.*, 2011).

5.4. Paleoearthquakes

In turn, we have direct geological data concerning the fault activity in the late Holocene. The paleoseismological analyses revealed surface fault rupture some time after the burying of the paleosol that was dated as 255 AD to 401 AD (minimum offset of *ca*. 40 cm on a secondary splay; Fig. 11, B). This date fits very well with the age of the penultimate earthquake that was identified in most of the Fucino trenches (Fig. 2) by Galadini and Galli (1999), who attributed it to the known 508 AD Rome earthquake (Galadini and Galli, 2001). A similar dating is also provided by Schlagenhauf *et al.* (2010, 2011), for their ultimate detectable events, a period for which we have excluded significant erosional exhumation of the *nastro*.

A further surface rupture affects all of the deposits in the trench, as shown by the splay cutting through the presently forming uppermost horizon, and by a vent that opened between the *nastro* and the talus, which is filled with organic material (Fig. 11, C, A, respectively). This event looks much less important in terms of offset/ deformation (i.e., Schlagenhauf *et al.*, 2010, were not able to define it). Thus it must be very recent, and we have attributed it to the 1915 Fucino earthquake. Its surficial trace appears to match with a vent reported by several newspapers in the days after this earthquake, although we have not found any more detailed description of this.

The trench also provides some indications concerning a previous faulting event(s) that have affected the Neoglacial colluvia (post 4.5 ka) that was sealed by an erosional surface that developed well before the deposits of the Roman period. The time span of this event matches roughly with that identified in the Fucino trenches as having occurred before the 508 AD earthquake [3500-3300 BP; i.e., 1450 BC in Galli *et al.* (2008)], and with the penultimate event of Schlagenhauf (2009) and Schlagenhauf *et al.* (2010), respectively [3.3 ±0.7 BP and 3.4 (+0.5/-0.9) BP].

5.5 Seismogenetic behavior

By taking into account the slip events identified through the paleoseismological analysis, we have hypothesized that the MF ruptured together with the other Fucino faults during both the 508 AD and the 1915 earthquakes (M_w 7), and perhaps in the 1450 BC earthquake, even though the 1915 surficial slip might have been smaller on the MF than in the High Middle Age event. Indeed, the western-most tip of the MF, which in January 2011 generated a Ml <4.0 swarm (Figs. 1, 2, NW-SE focal mechanism), probably ruptured also in the M_S 5.5 earthquake of 1904 (with the same epicenter as in 2011), reasonably for a length at depth of *ca*. 5 km (Figs. 1, 2). Therefore, on the one hand, this event anticipated the rupture of the entire Fucino fault system of 1915, while, on the other hand, it might have reduced the successive fault slip on the MF segment (and thus on the whole Fucino fault system, e.g., tentatively to 32 km; Fig. 13), and consequently the overall seismic energy that was released in 1915.

Thus, if in the 508 AD earthquake the entire Fucino fault system ruptured contemporarily (i.e., the whole 37-km-long Fucino structure), it probably released slightly greater energy than in 1915 (see the equivalent seismic moment values reported in Fig. 13). Indeed, in the 1915 event, the macroseismic effects in Rome were at VI-VII MCS (Molin *et al.*, 1999), whereas the damage recorded in 508 AD (Galli and Molin, in press) might tentatively account for a higher MCS, and

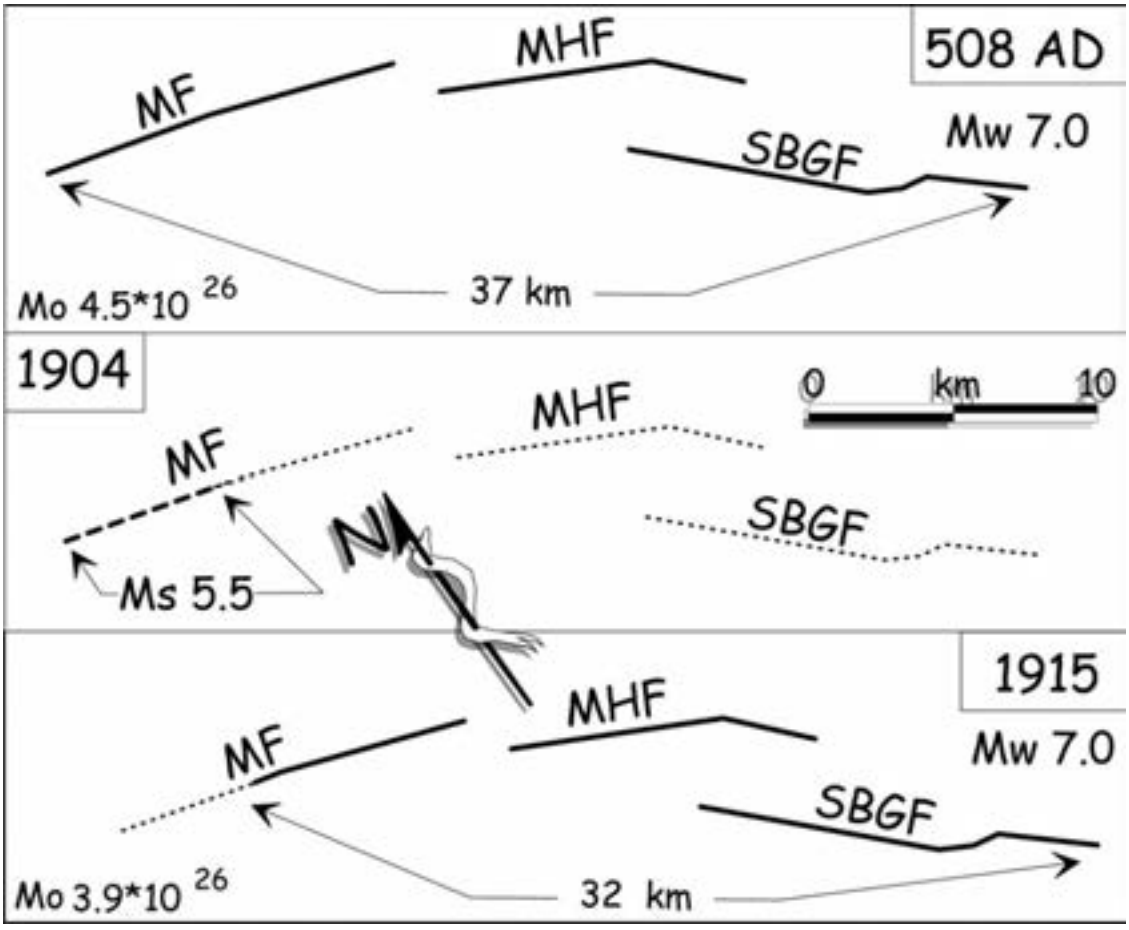

Fig. 13 - Hypothetical schemes of the Fucino fault system ruptures (bold lines) during the 508 AD (top), 1904 (middle) and 1915 (bottom) earthquakes. Fault labels as in Fig. 1. The seismic moment (M_o) and M_w are derived from the equation M_w = (log Mo/1.5) - 10.73 (dyne-cm). The 508 AD parameters were been calculated considering a 37-km-long fault. The bold dashed 1904 rupture means that this is not based on certain data.

thus a higher release of earthquake energy at the source (assuming the same NW-ward rupture directivity). This hypothesis, which makes no claims at being conclusive, is actually based on the effects recorded by a single building: i.e., the Flavian Amphitheatre (i.e., the Coliseum), which was still intact and in use in 508 AD, whereas it has been partly collapsed and despoiled by its structural elements (i.e., all of the iron clamps) since the Middle Ages. Nevertheless, the Coliseum was seriously damaged in 508 AD (Galli and Molin, in press), but not in 1915 (Molin *et al.*, 1995), when it appears that it should have been more vulnerable.

6. Conclusions

In the present study, we have constrained the Quaternary activity of the 15-km-long normal Magnola Fault, both over the long-term and the short-term. The slip rates calculated for the past

ca. 1 Ma are in the order of 0.6 mm/yr, whereas those for the past 30 ka (i.e., from the early beginning of the local LGM) lie between 0.3 mm/yr and 0.9 mm/yr. Considering the complex interaction between the climate-related fault exhumation *versus* the co-seismic surface slip, these are possibly close to 0.6 mm/yr, which is the same value as over the long-term. This accounts for a local extension rate of 0.4 mm/yr to 0.5 mm/yr, which when added to the similar values associated with both the Middle Aterno fault system and the Campo Imperatore fault system (Fig. 1), gives a fault-controlled regional extension of about half of that evaluated through the GPS analyses of D'Agostino *et al.* (2011) in this sector of the Apennines.

The paleoseismic analyses performed in a single trench have been compared to those already published in the area, allowing us to hypothesize that the MF ruptured in both the 508 AD and 1915 earthquakes, with the latter being anticipated by a large foreshock in 1904 that probably reduced the later release of seismic energy.

Our data suggest that as with many other fault segments that are part of the primary fault systems of the Apennines, the Magnola Fault can rupture both independently of the other segments of the Fucino fault system, which generates M_W <6.0 earthquakes (as in 1904, or larger if the entire 15-km-long of the MF should rupture), and together with the adjacent Fucino faults, which generates catastrophic earthquakes (such as those in 508 AD and 1915).

Acknowledgments. We are grateful to Stefano Solarino and to another anonymous reviewer for their useful criticism and suggestions. The views and conclusions contained here are those of the authors and should not be interpreted as necessarily representing official policies, either expressed or implied, of the Italian Government.

REFERENCES

Amato A., Galli P. and Mucciarelli M.; 2011: *Introducing the special issue on the 2009 L'Aquila earthquake*. Boll. Geof. Teor. Appl., **52**, 357-365, doi: 10.4430/bgta0033.

Bagh S., Chiaraluce L., De Gori P., Moretti M., Govoni A., Chiarabba C., Di Bartolomeo P. and Romanelli M.; 2007: *Background seismicity in the Central Apennines of Italy: the Abruzzo region case study*. Tectonophys., **444**, 80-92.

Bartolini C.; 2010: *Il ruolo morfogenetico della tettonica è sopravvalutato?* In: Slejko D. e Riggio A. (ed), Gruppo Nazionale di Geofisica della Terra Solida, 29° Convegno Nazionale, Riassunti estesi delle comunicazioni. Stella Arti Grafiche, Trieste, pp. 13-14.

Berardi R., Contri P., Galli P., Mendez A. and Pacor F.; 1999: *Modellazione degli effetti di amplificazione locale nelle città di Avezzano, Ortucchio e Sora.* In: Castenetto S. and Galadini F. (eds), 13 gennaio del 1915. Il terremoto nella Marsica, Servizio Sismico Nazionale, pp. 349-372.

Bertini T. and Bosi C.; 1993: *La tettonica quaternaria della conca di Fossa (L'Aquila).* Il Quaternario, **6**, 293-314.

Boncio P., Lavecchia G. and Pace B.; 2004: *Defining a model of 3D seismogenic sources for seismic hazard assessment applications: the case of central Apennines (Italy).* J. Seismolog., **8**, 407-425.

Bosi C.; 1975: *Osservazioni preliminari su faglie probabilmente attive nell'Appennino centrale.* Boll. Soc. Geol. It., **94**, 827-859.

Bosi C. and Messina P.; 1991: *Ipotesi di correlazione fra successioni morfolitostratigrafiche pliopleistoceniche nell'Appennino laziale-abruzzese.* Studi Geol. Camerti, 1991, 257-263.

Bosi C., Galadini F., Giaccio B., Messina P. and Sposato A.; 2003: *Plio-quaternary continental deposits in the latium-abruzzi Apennines: the correlation of geological events across different intermontane basins.* Il Quaternario, **16**, 55-76.

Bosi V., Funiciello R. and Montone P.; 1994: *Fault inversion: an example in Central Apennines (Italy).* Il Quaternario, **7**, 577-588.

Castiglioni G.B.; 1979: *Geomorfologia*. UTET, Torino, 436 pp.

Cello G., Mazzoli S., Tondi E. and Turco E.; 1997: *Active tectonics in the Central Apennines and possible implications for seismic hazard analysis in peninsular Italy.* Tectonophys., **272**, 43-68.

Chiarini E., Messina P. and Papasodaro F.; 1997: *Evoluzione geologica e tettonica plioquaternaria dell'alta valle del F. Salto (Italia centrale). Primi risultati derivanti dall'analisi delle superfici relitte e dei depositi continentali.* Il Quaternario, **10**, 625-630.

Clark P.U., Dyke A.S., Shakun J.D., Carlson A.E., Clark J., Wohlfarth B., Mitrovica J.X., Hostetler S.W. and McCabe M.A.; 2009: *The last glacial maximum.* Science, **325**, 710-714, doi:10.1126/science.1172873.

Corriere d'Italia, 20/01/1915.

Corriere di Napoli, 21/01/1915.

D'Agostino N., Mantenuto S., D'Anastasio E., Giuliani R., Mattone M., Calcaterra S., Gambino P. and Bonci L.; 2011: *Evidence for localized active extension in the central Apennines (Italy) from global positioning system observations.* Geology, **39**, 291-294, doi:10.1130/ G31796.1.

D'Agostino N., Speranza F. and Funiciello R.; 1997: *Le brecce Mortadella dell'Appennino Centrale: primi risultati di stratigrafia magnetica*. Il Quaternario, **10**, 385-388.

Demangeot J.; 1965: *Geomorphologie des Abruzzes adriatiques.* Cartographiques Memoires et Documents, Centre Recherche et Documentation, Paris, France, 403 pp.

Dramis F.; 1983: *Morfogenesi di versante nel Pleistocene superiore in Italia: idepositi detritici stratificati.* Geogr. Fis. Din. Quat., **6**, 180-182.

Erhart H.; 1951: *La genèse des sols en tant que phénomène géologique.* Esquisse d'une théorie géologique et géochimique. Biostasie et rhéxistasie. Masson, Paris, 90 pp.

Font M., Lagarde J.-L., Amorese D., Coutard J.-P., Dubois A., Guillemet G., Ozouf J.-C. and Vedie E.; 2006: *Physical modelling of fault scarp degradation under freeze/thaw cycles.* Earth Surf. Processes Landforms, **31**, 1731-1745.

Frezzotti M. and Giraudi C.; 1992: *Evoluzione geologica tardo-pleistocenica ed olocenica del conoide di Valle Majelama (Massiccio del Velino, Abruzzo).* Il Quaternario, **5**, 33-50.

Galadini F.; 2006: *Quaternary tectonics and large-scale gravitational deformations with evidence of rock-slide displacements in the Central Apennines (central Italy).* Geomorphol., **82**, 201-228.

Galadini F. and Galli P.; 1999: *The Holocene paleoearthquakes on the 1915 Avezzano earthquake faults (central Italy): Implications for active tectonics in Central Apennines.* Tectonophys., **308**, 143-170.

Galadini F. and Galli P.; 2000: *Active tectonics in the central Apennines (Italy) - input data for seismic hazard assessment.* Nat. Hazards, **22**, 225-270.

Galadini F. and Galli P.; 2001: *Archeoseismology in Italy: Case studies and implication on long- term seismicity*. J. Earthquake Eng., **5**, 35-68.

Galadini F., Galli P. and Giraudi C.; 1997: *Paleosismologia della Piana del Fucino (Italia Centrale).* Il Quaternario, **10**, 27-64.

Galadini F., Galli P. and Giraudi C.; 1999: *Gli effetti geologici del terremoto del 1915.* In: Castenetto S. and Galadini F. (eds), "13 gennaio del 1915. Il terremoto nella Marsica", Servizio Sismico Nazionale, pp. 283-300.

Galadini F., Galli P., Giraudi C. and Molin D.; 1995: *Il terremoto del 1915 e la sismicità della Piana del Fucino (Italia Centrale).* Boll. Soc. Geol. It., **114**, 635-663.

Galadini F., Galli P. and Molin D.; 1998: *Caratteristiche della sismicità della zona del Fucino (Italia centrale): Implicazioni sismotettoniche*. Il Quaternario, **11**, 179-189.

Galli P. and Galadini F.; 2003: Disruptive earthquakes revealed by faulted archaeological relics in Samnium (Molise, southern Italy). Geophys. Res. Lett., **30**, 1266, doi: 10.1029/2002GL016456.

Galli P. and Molin D.; 2012: *Beyond the damage threshold: the historic earthquakes of Rome.* Bull. Earthquake Engineering, in press.

Galli P. and Naso G.; 2009: *Unmasking the 1349 earthquake source (southern Italy).* Paleoseismological and archaeoseismological indications from the Aquae Iuliae fault. J. Struct. Geol., **31**, 128-149.

Galli P., Bosi V., Piscitelli S., Giocoli A. and Scionti V.; 2006: *Late Holocene earthquakes in southern Apennines: paleoseismology of the Caggiano fault.* Int. J. Earth Sciences, **95**, 855-870.

Galli P., Carducci T., Esposito E., Naso G., Peronace E. and Quadrio B.; 2010a: *Earthquakes and fault(s) in the Upper Ofanto Valley (Irpinia, southern Italy).* Rend. Online Soc. Geol. It., **11**, 21-22.

Galli P., Esposito G., Naso G., Peronace E. and Quadrio B.; 2010b: *New paleoseismic clues along the Mount Marzano fault system (southern Apennine).* In: Slejko D. e Riggio A. (ed), Gruppo Nazionale di Geofisica della Terra Solida, 29° Convegno Nazionale, Riassunti estesi delle comunicazioni. Stella Arti Grafiche, Trieste, pp. 64-66.

Galli P., Galadini F. and Calzoni F.; 2005: *Surface faulting in Norcia (central Italy): a "paleoseismological perspective".* Tectonophys., **403**, 117-130.

Galli P., Galadini F. and Pantosti D.; 2008: *Twenty years of paleoseismology in Italy.* Earth Sci. Rev., **88**, 89-117.

Galli P., Giaccio B. and Messina P.; 2010c: *The 2009 central Italy earthquake seen through 0.5 Myr-long tectonic history of the L'Aquila faults system.* Quat. Sci. Rev., **29**, 3768-3789, doi:10.1016/j.quascirev.2010.08.018.

Galli P., Giaccio B., Messina P. and Peronace E.; 2011: *Paleoseismology of the L'Aquila faults (central Italy, 2009 M_w 6.3 earthquake).* Clues on active fault linkage. Geophys. J. Int., **187**, 1119-1134, doi:10.1111/J.1365-246X.2011.05233.x.

Galli P., Orsini G., Bosi V., Di Pasquale G. and Galadini F.; 2002: *Testing damage scenarios. From historical earthquakes to silent active faults.* In: Proc. EGS XXVII General Assembly, Nice, France, Abstract 03979.

Gasparini C., Iannaccone G. and Scarpa R.; 1985: *Fault-plane solutions and seismicity of the Italian Peninsula.* Tectonophys., **117**, 59-78.

Gazzetta del Popolo, 21/01/1915.

Giaccio B., Galli P., Messina P., Jicha B., Scardia G., Falcucci E., Galadini F., Gori S., Peronace E., Sottili G., Sposato A. and Zuppi G.M.; 2011: *Roaming fault activity and basin depocentre shifting in the L'Aquila 2009 mesoseismic region (central Apennine) over the last 2 Ma.* In: In: Slejko D. e Rebez A. (ed), Gruppo Nazionale di Geofisica della Terra Solida, 30° Convegno Nazionale, Riassunti estesi delle comunicazioni. Moretti Tecniche Grafiche, Trieste, pp. 54-57.

Giraudi C.; 2004: *The Apennine glaciations in Italy.* In: Ehlers J. and Gibbard P.L. (eds), Quaternary Glaciations-Extent and Chronology, Elsevier, Amsterdam, Netherland, pp. 215-224.

Giraudi C., Magny M., Zanchetta G. and Drysdale R.N.; 2011: *The Holocene climatic evolution of Mediterranean Italy: A review of the continental geological data.* The Holocene, **21**, 105-115.

Gori S., Dramis F., Galadini F. and Messina P.; 2007: *The use of geomorphological markers in the footwall of active faults for kinematic evaluations: examples from the central Apennines.* Boll. Soc. Geol. It., **126**, 365-374.

Il Giornale d'Italia, 16/03/1904.

Il Mattino, 21-22/01/1915.

Margottini C. and Screpanti A.; 1999: *Attribuzione della magnitudo al terremoto di Avezzano del 13 gennaio 1915 e studio dell'evoluzione temporale della crisi sismica associata.* In: Castenetto S. and Galadini F. (eds), "13 gennaio del 1915. Il terremoto nella Marsica", Servizio Sismico Nazionale, pp. 301-318.

Margottini C., Ambraseys N.N. and Screpanti A.; 1993: *La magnitudo dei terremoti italiani del XX secolo*. ENEA, Roma, 57 pp.

Martín-Puertas C., Valero-Garcés,B.L., Brauer A., Mata M.P., Delgado-Huertas A. and Dulski P.; 2009: *The Iberian-Roman Humid Period (2600-1600 cal yr BP) in the Zoñar Lake varve record (Andalucía, southern Spain)*. Quaternary Research, **71**, 108-120.

Messina P., Galli P. and Giaccio B.; 2011a: *Comment on 'Insights from the M_w 6.3, 2009 L'Aquila earthquake (central Apennines) to unveil new seismogenic sources through their surface signature: the adjacent San Pio Fault*. Terranova, **23**, 280-282, doi:10. 1111/j.1365-3121.2011.01010.x.

Messina P., Galli P. and Giaccio B.; 2011b: *The Quaternary evolution of the San Pio basin and the progressive extintion of its bounding fault (L'Aquila, central Apennines).* In: Slejko D. e Rebez A. (ed), Gruppo Nazionale di Geofisica della Terra Solida, 30° Convegno Nazionale, Riassunti estesi delle comunicazioni. Mosetti Tecniche Grafiche, Trieste, pp. 65-69.

Michetti A.M., Brunamonte F., Serva L. and Vittori E.; 1996: *Trench investigations of the 1915 Fucino earthquake fault scarps (Abruzzo, Central Italy): geological evidence of large historical events.* J. Geophys. Res., **101**, 5921-5936, doi:10.1029/95J B02852.

Molin D., Castenetto S., Di Loreto E., Guidoboni E., Liperi L., Narcisi B., Paciello A., Riguzzi F., Rossi A., Tertulliani A. and Traina G.; 1995: *Sismicità di Roma.* In: Funiciello R. (ed), Mem. Descr. Carta Geol. It., **50**, 323-408.

Molin D., Galadini F., Galli P., Mucci L. and Rossi A.; 1999: *Terremoto del Fucino del 13 gennaio 1915 - Studio macrosismico.* In: Castenetto S. and Galadini F. (eds), "13 gennaio del 1915. Il terremoto nella Marsica", Servizio Sismico Nazionale, pp. 321-340.

Murton J.B., Peterson R. and Ozouf J.C.; 2006: *Bedrock fracture by ice segregation in cold regions.* Science, **314**, 1127-1129, doi10.1126/ science.1132127.

Nijman W.; 1971: *Tectonics of Velino-Sirente area, Abruzzi, Central Italy.* Proc. K. Ned. Akad. Wet., **74**, 156-184.

Oddone E. 1915: *Gli elementi fisici del grande terremoto marsicano fucense del 13 Gennaio 1915.* Boll. Soc. Sismol. It., **29**, 71-215.

Osservatore Romano, 21/01/1915.

Palumbo L., Benedetti L., Bourlès D., Cinque A. and Finkel R.; 2004: *Slip history of the Magnola fault (Apennines, Central Italy) from 36Cl surface exposure dating: Evidence for strong earthquake over Holocene*. Earth Planet. Sci. Lett., **225**, 163-176.

Patacca E., Scandone P., Di Luzio E., Cavinato G. and Parotto M.; 2008: *Structural architecture of the central Apennines: interpretation of the CROP 11 seismic profile from the Adriatic coast to the orographic divide.* Tectonics, **27**, TC3006, doi10.1029/2005TC 001917.

Peccerillo A.; 2005: *Plio-Quaternary Volcanism in Italy.* Springer-Verlag, Berlin, Heidelberg, 365 pp.

Piccardi L., Gaudemer Y., Tapponier P. and Boccaletti M.; 1999: *Active oblique extension in the central Apennines (Italy): evidence from the Fucino region.* Geophys. J. Int., **139**, 499-530.

Pondrelli S., Salimbeni S., Morelli A., Ekström G., Olivieri M. and Boschi E.; 2010: *Seismic moment tensors of the April 2009, L'Aquila (central Italy), earthquake sequence.* Geophys. J. Int., **180**, 238-242, doi: 10.1111/j.1365-246X.2009.04418.x.

Regione Abruzzo; 2010: *CTRN Regione Abruzzo 1:5000 - Carta Tecnica Regionale Numerica.* Regione Abruzzo, Italy.

Roberts G.P. and Michetti A.M.; 2004: *Spatial and temporal variations in growth rates along active normal fault systems: an example from the Lazio-Abruzzo Apennines, central Italy*. J. Struct. Geol., **26**, 339-376.

Schlagenhauf A.; 2009: *Identification des forts séismes passés sur les failles normales actives de la région Lazio-Abruzzo (Italie Centrale) par 'datations cosmogéniques' (36Cl) de leurs escarpements.* MSc Thesis, Université Joseph Fourier, Grenoble, France, 300 pp.

Schlagenhauf A., Gaudemer Y., Manighetti I., Palumbo L., Schimmelpfennig I., Finkel R. and Pou K.; 2010: *Using in situ Chlorine-36 cosmonuclide to recover past earthquake histories on limestone normal fault scarps: a reappraisal of methodology and interpretations.* Geophys. J. Int., **182**, 36-72, doi:10.1111/j.1365-246X.2010.04622.x.

Schlagenhauf A., Manighetti I., Benedetti L., Gaudemer Y., Finkel R., Malavieille J. and Pou K.; 2011: *Earthquake supercycles in Central Italy, inferred from 36Cl exposure dating.* Earth Planet. Sci. Lett., **307**, 487-500, doi10.1016/j.e psl.2011.05.022.

Serva L., Blumetti A.M. and Michetti A.M.; 1988: *Gli effetti sul terreno del terremoto del Fucino (13 Gennaio 1915); tentativo di interpretazione dell'evoluzione tettonica recente di alcune strutture.* Mem. Soc. Geol. It., **35**, 893-907.

Slemmons D.B.; 1957: *Geological effects of the Dixie Valley-Fairview Peak, Nevada, earthquakes of December 16, 1954.* Bull. Seismol. Soc. Am., **47**, 353-375.

SLU-EC; 2011: *Saint Luis University Earthquake center.* <http://www.eas.slu.edu/eqc/eqc_mt/MECH.IT/>, last access November 2011.

Spadea M.C., Vecchi M., Gardellini P. and Del Mese S.; 1985: *The Marsica earthquake of February 24, 1904.* In: Postpischl D. (ed), Atlas of isoseismal maps of Italian earthquakes, Quaderni della Ricerca Scientifica, **114**, 114-115.

Stuiver M., Reimer P.J. and Reimer R.; 2010: *CALIB Radiocarbon Calibration.* Execute Version 6.0html, <http://calib.qub.ac.uk/calib/>, last access November 2011.

Corresponding author: Paolo Galli
Dipartimento della Protezione Civile
Via Vitorchiano 4, 00189 Rome, Italy
Phone: +39 06 68204892; fax: +39 06 68202877; e-mail: paolo.galli@protezionecivile.it